The High-pressure Thallium Triborate HP-TlB_3O_5

Gerhard Sohr[a], Lukas Perfler[b] and Hubert Huppertz[a]

[a] Institut für Allgemeine, Anorganische und Theoretische Chemie, Leopold-Franzens-Universität Innsbruck, Innrain 80 – 82, A-6020 Innsbruck, Austria

[b] Institut für Mineralogie und Petrographie, Leopold-Franzens-Universität Innsbruck, Innrain 52f, A-6020 Innsbruck, Austria

Reprint requests to H. Huppertz. E-mail: Hubert.Huppertz@uibk.ac.at

Z. Naturforsch. **2014**, *69b*, 1260 – 1268 / DOI: 10.5560/ZNB.2014-4124
Received June 2, 2014

Dedicated to Professor Hubert Schmidbaur on the occasion of his 80th birthday

The thallium triborate HP-TlB_3O_5 (HP = high-pressure) was synthesized in a Walker-type multi-anvil apparatus under high-pressure/high-temperature conditions of 6 GPa and 1400°C. A mixture of thallium carbonate Tl_2CO_3 and boric acid H_3BO_3 initially heated at 850°C under ambient-pressure conditions was used as a precursor for the high-pressure experiment. Single-crystal X-ray diffraction data revealed that HP-TlB_3O_5 is isotypic to HP-$M'B_3O_5$ (M' = K, Rb). Furthermore the B–O network is identical to the substitutional variants HP-$M''B_3O_5$ [$M'' = Cs_{1-x}(H_3O)_x$ ($x = 0.5 - 0.7$), NH_4]. HP-TlB_3O_5 crystallizes with eight formula units ($Z = 8$) in the monoclinic space group $C2/c$ (no. 15). The lattice parameters are $a = 996.3(2)$, $b = 884.0(2)$, $c = 913.1(2)$ pm, $\beta = 103.3(1)°$, and $V = 782.5(3)$ Å^3. Trigonal-planar BO_3 groups, corner-sharing BO_4 tetrahedra, and B_2O_6 groups consisting of two edge-sharing BO_4 tetrahedra are present in the structure, forming a three-dimensional network. The thallium ions are located in channels of the boron-oxygen network being tenfold coordinated by oxygen atoms and do not show any lone pair effect at all. IR and Raman spectroscopic investigations were performed on single crystals of the compound.

Key words: High-pressure, Borate, Crystal Structure, Lone Pair, Thallium

Introduction

Since the publication of $KZnB_3O_6$ [1 – 3], we focused our research on the syntheses of high-pressure alkali metal borates. $KZnB_3O_6$ was the first example of two borates synthesized under ambient-pressure conditions exhibiting the structural motive of edge-sharing BO_4 tetrahedra [3, 4]. At that time, all other compounds containing edge-sharing BO_4 tetrahedra were high-pressure phases, *e. g.* $RE_4B_6O_{15}$, (*RE* = Dy, Ho) [5], α-$RE_2B_4O_9$ (*RE* = Sm, Eu, Gd, Tb, Ho) [6, 7], HP-MB_2O_4 (*M* = Ni, Co) [8, 9], β-FeB_2O_4 [10], and $Co_7B_{24}O_{42}(OH_2) \cdot 2\,H_2O$ [11]. Interestingly, any high-pressure alkali metal borates were known to literature. Since then, we successfully synthesized high-pressure borates of all alkali metal cations represented by the compounds HP-LiB_3O_5 [12], HP-$Na_2B_4O_7$ [13], HP-MB_3O_5 (*M* = K, Rb) [14, 15], and HP-CsB_5O_8 [16]. During the systematic scanning of the system Cs-B-O, we discovered HP-$Cs_{1-x}(H_3O)_xB_3O_5$ ($x = 0.5 - 0.7$) which is the first borate containing oxonium ions [17]. This finding proves that alkali metal cations can be substituted by pseudo alkali metal ions like H_3O^+ in high-pressure borates. With the substitutional variant HP-$(NH_4)B_3O_5$, we recently synthesized a high-pressure borate containing solely the pseudo alkali metal cation NH_4^+ [18]. Another pseudo alkali metal cation is thallium(I). In contrast to the above mentioned alkali and pseudo alkali metal cations, it has two valence electrons left forming a lone pair. Depending on the surrounding of the Tl^+ ion, this lone pair can either be stereochemically active or inactive [19].

Up to now, eleven phases are known in the system Tl-B-O, but only five of them have been examined structurally. One of them, TlB_5O_8, is the only one without a lone pair effect [20]. The normal-pressure compound TlB_3O_5 is built up from B_3O_3 rings which are linked to each other by bridging oxygen atoms to form a three-dimensional framework. A small lone pair effect is observed in its stucture [21]. In contrast, β-

$Tl_2B_4O_7$, $TlBO_2$ and Tl_3BO_3 show a remarkably stereochemically active lone pair [19, 22, 23]. The compounds α- and γ-$Tl_2B_4O_7$ [24, 25] have been characterized by powder diffraction only, as well as $Tl_2B_8O_{13}$ and the high-pressure phase $TlBO_3$ [21, 26]. Furthermore, TlB_9O_{14} and $Tl_4B_2O_5$ are stated, but no crystallographic proof is given [25, 27].

This work presents the new thallium triborate HP-TlB_3O_5. The compound was synthesized under high-pressure conditions and characterized by powder and single-crystal X-ray diffraction as well as by IR and Raman spectroscopy. Its structure and the vibrational spectra are discussed in comparison with the isotypic phases HP-$M'B_3O_5$ ($M' =$ K, Rb) and the substitution variants HP-$M''B_3O_5$ [$M'' = Cs_{1-x}(H_3O)_x$ ($x = 0.5-0.7$), NH_4]. Furthermore, the effect of the lone pair is examined.

Experimental Section

Synthesis

HP-TlB_3O_5 was synthesized in two steps during a systematic scan of the system Tl-B-O. First, an ambient-pressure/high-temperature synthesis was carried out. A stoichiometric educt mixture of 0.7400 g (1.5786 mmol) Tl_2CO_3 (99.995 %, Alfa Aesar, Karlsruhe, Germany) and 0.5857 g (9.4723 mmol) H_3BO_3 (99.5 %, Carl Roth, Karlsruhe, Germany) was ground together in an agate mortar and filled into an FKS 95/5 (Feinkornstabilisiert, 95 % Pt, 5 % Au) crucible (no. 21, Ögussa, Vienna, Austria). The mixture was heated to 600°C in 6 h and kept at this temperature for 4 h. Further heating up to 850°C lasted 3 h. After holding the temperature for 36 h, the mixture was quenched to room temperature. The resulting product was finely ground, filled into a crucible made of hexagonal boron nitride (HeBoSint®

Table 1. Crystal data and structure refinement of HP-TlB_3O_5 (standard deviations in parentheses).

Empirical formula	HP-TlB_3O_5
Molar mass, g mol^{-1}	316.80
Crystal system	monoclinic
Space group	$C2/c$ (no. 15)
Powder diffractometer	Stoe Stadi P
Radiation; wavelength, pm	Mo$K_{\alpha1}$; $\lambda = 70.930$
Powder data	
a, pm	996.26(6)
b, pm	883.91(6)
c, pm	913.01(6)
β, deg	103.30(1)
V, Å^3	782.4(1)
Single-crystal diffractometer	Enraf-Nonius Kappa CCD
Radiation; wavelength, pm	MoK_α; $\lambda = 71.073$
Single-crystal data	
a, pm	996.3(2)
b, pm	884.0(2)
c, pm	913.1(2)
β, deg	103.3(1)
V, Å^3	782.5(3)
Formula units per cell, Z	8
Calculated density, g cm^{-3}	5.38
$F(000)$, e	1088
Crystal size, mm^3	$0.07 \times 0.06 \times 0.02$
Temperature, K	293(2)
Absorption coefficient, mm^{-1}	41.2
θ range, deg	3.1 – 37.8
Range in hkl	$-17 \le h \le 16$, $-15 \le k \le 15$, $-15 \le l \le 15$
Total no. of reflections	7287
Absorption correction	multi-scan [33]
Independent reflections / R_{int} / R_σ	2093 / 0.0893 / 0.0709
Reflections with $I > 2\,\sigma(I)$	1376
Data/refined parameters	2093 / 83
Goodness-of-fit on F_i^2	1.042
Final $R1$ / $wR2$ [$I > 2\,\sigma(I)$]	0.0477 / 0.0818
$R1$ / $wR2$ (all data)	0.0477 / 0.0818
Largest diff. peak/hole, e Å^{-3}	2.66 / −4.52

P100, Henze BNP GmbH, Kempten, Germany), and compressed by eight tungsten carbide cubes (HA-7 %Co, Hawedia, Marklkofen, Germany) *via* an 18/11-assembly. A hydraulic press (mavo press LPR 1000-400/50, Max Voggenreiter GmbH, Mainleus, Germany) and a Walker-type module (also Max Voggenreiter GmbH) were used to apply the pressure. The assembly and its preparation are described in the references [28 – 31]. The compression of the precursor to 6 GPa lasted 3 h. At this pressure, the sample was heated to 1400°C within 10 min and kept there for 10 min. After cooling to 800°C within 5 h, the heating was turned off to quench the reaction mixture to room temperature. The decompression of the assembly lasted 9 h.

The sample was separated from the surrounding octahedral pressure medium (MgO, Ceramic Substrates & Components Ltd., Newport, Isle of Wight, UK) and removed from the boron nitride crucible. The sample consisted of colorless crystals, which were found to be HP-TlB_3O_5. Under air, brown dots formed on the surface of the crystals.

Crystal structure analysis

To measure the powder X-ray diffraction pattern of HP-TlB_3O_5, a Stoe Stadi P powder diffractometer with Ge(111)-monochromatized $MoK_{\alpha 1}$ radiation ($\lambda = 70.93$ pm) was used in transmission geometry. Fig. 1 shows the experimental powder pattern of HP-TlB_3O_5 matching well with the theoretical pattern simulated from the single-crystal data. A minute amount of hexagonal BN originating from the crucible is visible at $2\nu = 12.235°$. 92 reflections of the powder pattern were indexed and refined [32]. The lattice parameters fit well with the lattice parameters obtained from the single-crystal data (see Table 1). Single crystals of HP-TlB_3O_5 were selected by polarization contrast microscopy and isolated by mechanical fragmentation. Collection of the single-crystal intensity data using a Nonius Kappa-CCD diffractometer with graphite-monochromatized MoK_α radiation ($\lambda = 71.073$ pm) was conducted at room temperature. A semi-empirical absorption correction based on equivalent and redundant intensities (SCALEPACK [33]) was applied to the intensity data. From the systematic extinctions, the space groups $C2/c$ and Cc were derived. With the lattice parameters being comparable to those of HP-$M'B_3O_5$ ($M' = $ K, Rb) and HP-$M''B_3O_5$ ($M'' = Cs_{1-x}(H_3O)_x$ ($x = 0.5 - 0.7$), NH_4), the positional parameters of HP-KB_3O_5 were used as starting values for the refinement of the structure in the monoclinic space group $C2/c$, since the two phases are isotypic. All atoms were refined with anisotropic displacement parameters, and the final difference Fourier syntheses did not re-

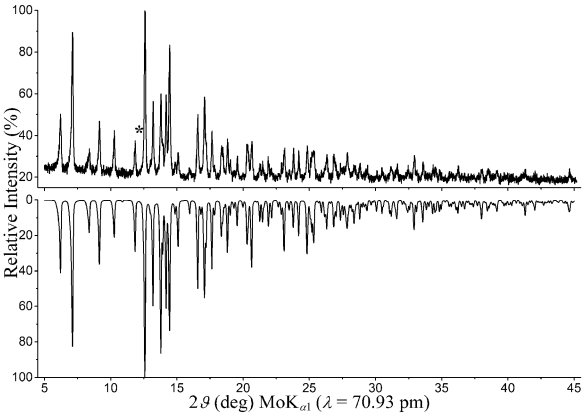

Fig. 1. Experimental powder pattern of HP-TlB_3O_5 (top), compared with the theoretical powder pattern (bottom) simulated from single-crystal data. The reflection marked with an asterisk is caused by hexagonal boron nitride of the crucible.

Table 2. Atomic coordinates and equivalent isotropic displacement parameters U_{eq} (Å^2) of HP-TlB_3O_5 (space group: $C2/c$) with standard deviations in parentheses. U_{eq} is defined as one third of the trace of the orthogonalized U_{ij} tensor. All atoms lie on Wyckoff positions $8f$.

Atom	x	y	z	U_{eq}
Tl1	0.08024(3)	0.34881(3)	0.44019(3)	0.02355(6)
O1	0.0791(4)	0.0116(5)	0.0980(5)	0.0091(7)
O2	0.1560(4)	0.0597(5)	0.3675(5)	0.0099(8)
O3	0.2498(4)	0.3512(5)	0.2475(5)	0.0111(7)
O4	0.3090(4)	0.0979(5)	0.1966(5)	0.0103(7)
O5	0.4108(5)	0.3040(5)	0.0978(5)	0.0124(8)
B1	0.1995(7)	0.0100(7)	0.2338(7)	0.009(2)
B2	0.3192(7)	0.2526(7)	0.1797(7)	0.009(2)
B3	0.4269(7)	0.4625(6)	0.0671(7)	0.007(2)

Atom	U_{11}	U_{22}	U_{33}	U_{12}	U_{13}	U_{23}
Tl1	0.0257(2)	0.0208(2)	0.0282(2)	−0.0015(2)	0.01449(9)	0.0019(2)
O1	0.007(2)	0.010(2)	0.010(2)	−0.002(2)	0.001(2)	0.002(2)
O2	0.013(2)	0.009(2)	0.008(2)	−0.003(2)	0.004(2)	−0.002(2)
O3	0.015(2)	0.009(2)	0.013(2)	−0.001(2)	0.010(2)	−0.003(2)
O4	0.012(2)	0.009(2)	0.014(2)	−0.003(2)	0.011(2)	−0.003(2)
O5	0.016(2)	0.006(2)	0.017(2)	0.001(2)	0.008(2)	−0.001(2)
B1	0.014(3)	0.003(2)	0.011(3)	0.002(2)	0.006(2)	0.001(2)
B2	0.009(2)	0.008(2)	0.012(2)	−0.000(2)	0.004(2)	0.000(2)
B3	0.008(2)	0.003(2)	0.010(2)	0.001(2)	0.004(2)	0.003(2)

Table 3. Anisotropic displacement parameters (Å^2) of HP-TlB_3O_5 (space group: $C2/c$) with standard deviations in parentheses.

Table 4. Interatomic distances (pm) in HP-TlB_3O_5 (space group: $C2/c$) calculated with the single-crystal lattice parameters (standard deviations in parentheses).

Tl1–O3	270.6(4)	B1–O4	144.3(8)	B2–O3	134.8(8)	B3–O2	141.6(8)
Tl1–O2	278.8(4)	B1–O2	145.4(8)	B2–O4	138.3(8)	B3–O5	144.5(7)
Tl1–O5	280.5(5)	B1–O3	148.8(7)	B2–O5	138.3(8)	B3–O1	151.2(8)
Tl1–O4	287.4(4)	B1–O1	151.4(8)			B3–O1	154.0(7)
Tl1–O2	291.8(4)	Ø B1–O	147.5	Ø B2–O	137.1	Ø B3–O	147.8
Tl1–O4	327.9(4)						
Tl1–O3	333.9(5)						
Tl1–O1	335.7(4)						
Tl1–O3	344.9(5)						
Tl1–O1	349.8(4)						
Ø Tl1–O	310.1					B3···B3	221(2)

Table 5. Bond angles (deg) in HP-TlB_3O_5 (standard deviations in parentheses).

O4–B1–O3	106.3(5)	O5–B2–O4	117.3(5)	O1–B3–O1	87.2(4)
O3–B1–O1	106.7(4)	O3–B2–O5	120.6(5)	O5–B3–O1	111.1(5)
O4–B1–O1	107.5(5)	O3–B2–O4	122.0(5)	O5–B3–O1	112.7(4)
O2–B1–O3	110.4(5)			O2–B3–O1	113.4(5)
O2–B1–O1	110.5(5)			O2–B3–O5	113.9(5)
O4–B1–O2	115.0(5)			O2–B3–O1	115.9(5)
Ø O–B1–O	109.4	Ø O–B2–O	120.0	Ø O–B3–O	109.0
				B3–O1–B3	92.8(4)

veal any significant peaks in the refinement (SHELXL-2013; full-matrix least-squares on F^2 [34 – 36]). All relevant details of the data collection and evaluation are listed in Table 1. Tables 2 – 5 show the positional parameters, anisotropic displacement parameters, selected interatomic distances, and bond angles, respectively.

Further details of the crystal structure investigation may be obtained from the Fachinformationszentrum Karlsruhe, D-76344 Eggenstein-Leopoldshafen, Germany (fax: +49-7247-808-666; e-mail: crysdata@fiz-karlsruhe.de, http://www.fiz-karlsruhe.de/request_for_deposited_data.html) on quoting the deposition number CSD-427689.

Vibrational spectroscopy

The transmission FT-IR spectra of single crystals of HP-TlB_3O_5 were measured in the spectral range of 600 – 5800 cm^{-1} with a Bruker Vertex 70 FT-IR spectrometer (spectral resolution 4 cm^{-1}), equipped with an MCT (*M*ercury *C*admium *T*elluride) detector and attached to a Hyperion 3000 microscope. As mid-infrared source, a Globar (silicon carbide) rod was used. 32 scans of the sample were acquired using a BaF_2 sample holder.

The single-crystal Raman spectrum of HP-TlB_3O_5 was measured in the spectral range of 100 – 1800 cm^{-1} with a Raman micro-spectrometer LabRAM HR-800 (HORIBA JOBIN YVON) and hundredfold magnification, using a frequency-doubled Nd:YAG laser ($\lambda = 532.22$ nm) as excitation source. The length of the crystal was approximately 0.05 mm. The Raman-scattered light was detected through an optical grid with 1800 lines/mm. Three ranges were measured with a spectral resolution better than 2 cm^{-1}. The measurement time per range was 10 s. A background correction was applied [37].

Results and Discussion

Synthesis conditions

HP-TlB_3O_5 could be synthesized over a wide range of starting compositions (molar ratio $Tl_2CO_3 : H_3BO_3$ from 1 : 1 – 1 : 12). It was formed at pressures between 6 and 12.5 GPa and at temperatures of 900 – 1400°C. The crystal quality increased with rising temperatures and decreased with rising pressure during the syntheses. Single crystals suitable for single-crystal diffraction experiments were obtained at 6 GPa by slow cooling from 1400°C to 800°C. Presumably, the crystal quality ameliorates further at higher temperatures, however these temperatures were not accessible using graphite as a furnace material.

Crystal structure of HP-TlB_3O_5

HP-TlB_3O_5 crystallizes with eight formula units per unit cell ($Z = 8$) in the monoclinic space group $C2/c$ (no. 15). The lattice parameters are $a = 996.3(2)$, $b = 884.0(2)$, $c = 913.1(2)$ pm, $\beta = 103.3(1)°$, and $V = 782.5(3)$ Å^3. The structure is built up from trigonal-planar BO_3 groups, corner-sharing BO_4 tetrahedra, and B_2O_6 groups consisting of two edge-sharing BO_4 tetrahedra (see Fig. 2). The phase is isotypic to

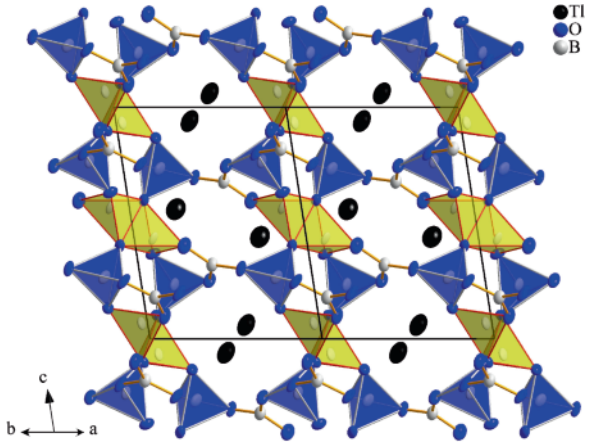

Fig. 2 (color online). Projection of the crystal structure of HP-TlB_3O_5 down [110]. Spheres: 90 % displacement ellipsoids. Dark polyhedra: corner-sharing BO_4 tetrahedra; light polyhedra: edge-sharing BO_4 tetrahedra.

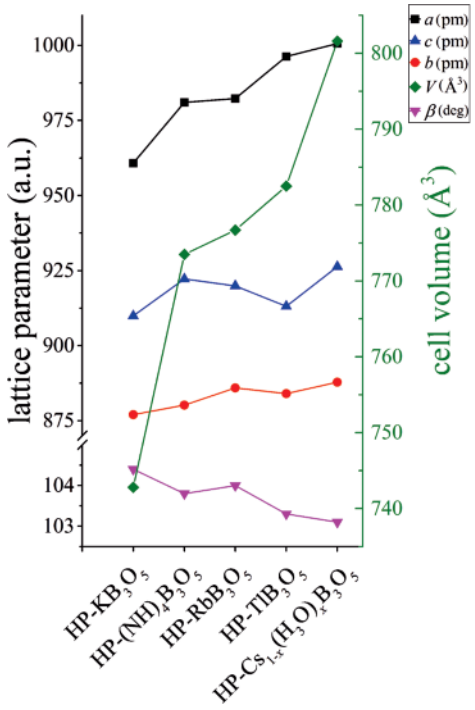

Fig. 3 (color online). Lattice parameters of the phases HP-MB_3O_5 [M = K, NH_4, Rb, Tl, $Cs_{1-x}(H_3O)_x$ ($x = 0.6$)].

HP-$M'B_3O_5$ (M' = K, Rb) [14, 15]. Two other compounds, HP-$Cs_{1-x}(H_3O)_xB_3O_5$ ($x = 0.5-0.7$) [17] and HP-$NH_4B_3O_5$ [18], represent substitution variants. A more detailed description of the crystal structure can be found in reference [14]. Table 6 presents a comparison of the isotypic phases and the substitution variants with respect to the unit cells, the coordination numbers of the alkali metal ions, the B–O bond lengths, and the O–B–O bond angles. The lattice parameters are graphically compared in Fig. 3. The volume of the unit cell slightly increases in the series HP-MB_3O_5 (M = K, NH_4, Rb, Tl, $Cs_{1-x}(H_3O)_x$ ($x = 0.6$)) parallel to the increase of the lattice parameters a, b and c, while the monoclinic angle β tends to decrease. The coordination numbers of the specific atoms as well as their connection patterns are identical.

The mean value of the B–O bond lengths and the O–B–O bond angles within the trigonal-planar BO_3 groups are 137.1 pm and 120.0°, respectively. In HP-TlB_3O_5, the BO_3 group is slightly distorted with B–O distances between 134.8(8) and 138.3(8) pm and angles from 117.3(5) to 122.0(5)°. The B–O bond lengths and angles within the corner-sharing tetrahedra of HP-TlB_3O_5 distribute from 144.3(8) to 151.4(8) pm (av. 147.5 pm) and from 106.3(5) to 115.0(5)° (av. 109.4°), respectively. With distances of 141.6(8) – 154.0(7) pm (av. 147.8 pm) and angles of 87.2(4)–115.9(5)° (av. 109.0°), the edge-sharing tetrahedra show a strong distortion which is typical for BO_4 tetrahedra forming a B_2O_6 group. This distortion is caused by the electrostatic repulsion of the two B^{3+} ions in the centers of the tetrahedra forming the B_2O_6 group [15]. The distance between the two boron cations B···B in HP-TlB_3O_5 amounts to 221(2) pm. Compared to other phases containing edge-sharing tetrahedra, *e. g.* α-$Eu_2B_4O_9$ (205.3(9) pm) or HP-NiB_2O_4 (208.8(2) pm), the B···B distances in the phases HP-MB_3O_5 (M = K, Rb, $Cs_{1-x}(H_3O)_x$ ($x = 0.5-0.7$), NH_4, Tl) are remarkably long. This is caused by two threefold-coordinated oxygen atoms at the common edge of the B_2O_6 group, which induce a scissor motion of the bond angles while the B–O bond lengths are unchanged. All values of the B–O distances and O–B–O angles as well as the values for the distances B···B in HP-TlB_3O_5 fit in well with the values in the other phases with the composition HP-MB_3O_5 [14, 15, 17, 18].

The boron-oxygen network forms channels down [110] incorporating the thallium atoms. They are tenfold coordinated by oxygen atoms with interatomic distances between 270.6(4) and 349.8(4) pm (av. 310.1 pm) (Fig. 4). The next oxygen ligand has a dis-

Table 6. Comparison of the structures HP-MB_3O_5 [M = K, NH_4, Rb, Tl, $Cs_{1-x}(H_3O)_x$ ($x = 0.6$)].

Empirical formula	HP-KB_3O_5	HP-RbB_3O_5	HP-$Cs_{1-x}(H_3O)_xB_3O_5$	HP-$(NH_4)B_3O_5$	HP-TlB_3O_5
Molar mass, g mol^{-1}	151.53	197.90	177.01	130.47	316.80
Unit cell dimensions					
a, pm	960.8(2)	982.3(2)	1000.6(2)	981.0(2)	996.3(2)
b, pm	877.0(2)	885.9(2)	887.8(2)	880.2(2)	884.0(2)
c, pm	909.9(2)	919.9(2)	926.3(2)	922.2(2)	913.1(2)
β, deg	104.4(1)	104.0(1)	103.1(1)	103.8(1)	103.3(1)
V, nm^3	0.7428(3)	0.7767(3)	0.8016(3)	0.7735(3)	0.7825(3)
Coordination number (CN)					
M (M = K, Rb, Cs, Tl)	10	10	11	–	10
Interatomic distances					
B1–O_{min}, pm	144.7(2)	144.3(3)	145.4(2)	145.7(2)	144.3(8)
B1–O_{max}, pm	152.4(2)	152.3(3)	152.1(2)	151.8(2)	151.4(8)
B1–$O_{average}$, pm	147.5	147.6	147.7	147.5	147.5
B2–O_{min}, pm	137.1(2)	136.9(3)	136.3(2)	136.1(2)	134.8(8)
B2–O_{max}, pm	137.9(2)	137.4(3)	138.2(2)	138.2(2)	138.3(8)
B2–$O_{average}$, pm	137.3	137.2	137.1	137.1	137.1
B3–O_{min}, pm	141.2(1)	141.5(3)	142.3(2)	142.1(2)	141.6(8)
B3–O_{max}, pm	154.8(1)	154.6(3)	154.7(2)	153.9(2)	154.0(7)
B3–$O_{average}$, pm	148.0	148.4	148.5	148.1	147.8
Bond angles					
O–B1–O_{min}, deg	106.6(1)	106.9(2)	107.1(2)	107.0(1)	106.3(5)
O–B1–O_{max}, deg	114.3(1)	114.9(2)	114.7(2)	114.4(1)	115.0(5)
O–B1–$O_{average}$, deg	109.4	109.4	109.4	109.4	109.4
O–B2–O_{min}, deg	117.7(1)	118.0(2)	117.8(2)	117.6(1)	117.3(5)
O–B2–O_{max}, deg	121.8(1)	121.7(2)	122.2(2)	122.0(1)	122.0(5)
O–B2–$O_{average}$, deg	120.0	120.0	120.0	120.0	120.0
O–B3–O_{min}, deg	87.4(1)	86.8(2)	86.6(1)	87.1(1)	87.2(4)
O–B3–O_{max}, deg	115.6(1)	115.7(2)	115.7(2)	115.9(1)	115.9(5)
O–B3–$O_{average}$, deg	109.0	109.0	109.0	109.0	109.0
B3···$B3_{min}$, pm	221.5(1)	223.1(3)	223.5(3)	221.5(2)	221(2)
B3–O1–B3, deg	92.7(1)	93.2(2)	93.5(1)	92.9(1)	92.8(4)

tance of 377.6(4) pm. Two neighboring Tl^+ cations are 341.9(1) pm apart which is close compared to other thallium borates (Tl···Tl_{min} = 359.6(5) pm [23]–531.6(2) pm [20]). The coordination number of the thallium cations in HP-TlB_3O_5 is the highest in the system Tl-B-O ($CN_{min} = 3$ [23]; $CN_{max} = 9$ [20]). The shortest and longest Tl–O distances of the Tl^+ coordination sphere are the second largest within the system (Tl–O_{min} = 245(2) pm [19]–290.0(5) pm [20]; Tl–O_{max} = 286(4) pm [22]–358(4) pm [23]), while the average Tl–O distance (310.1 pm) is the largest (Tl–O_{av} = 258 pm [22]–309.8 pm [21]). The increased coordination number and the long average Tl–O bond length are in agreement with the high-pressure rules and justify the classification of HP-TlB_3O_5 as high-pressure phase [38].

Interestingly, there is no visible effect caused by the obviously stereochemically inactive lone pair. An inactive lone pair is also found in TlB_5O_8, while the lone pair in TlB_3O_5 shows a weak effect on the crystal structure. In all other crystalline thallium borates with known structures, the lone pair is stereochemically active. This finding agrees with the observation that the lone pair effect seems to be linked to the values of the shorter Tl–O bond lengths as stated in reference [19]. TlB_5O_8 and HP-TlB_3O_5 have the longest Tl–O_{min} distance and an inactive lone pair, followed by TlB_3O_5 which shows already a weak lone pair effect. Penin *et al.* [19] also found a correlation between the B/Tl ratio and the lone pair effect. HP-TlB_3O_5 and TlB_3O_5 have the same B/Tl ratio and are isotypic to the alkali metal borates HP-MB_3O_5 (M = K, Rb) and CsB_3O_5 [14, 15, 39], respectively, possessing any lone pair effect. However, a small lone pair effect is reported for the normal-pressure phase TlB_3O_5 which is not observed in HP-TlB_3O_5. This finding is inconsistent with the assumed correlation between the B/Tl ratio and the lone pair effect. Presumably, the influence of the

Atom	Tl1	B1	B2	B3	O1	O2	O3	O4	O5
$\sum Q$	1.08	3.03	3.00	3.02	−2.08	−2.01	−2.10	−2.14	−1.97
$\sum V$	0.98	2.99	2.97	3.05	−1.87	−2.08	−2.07	−2.00	−1.98

Table 7. Bond valence sums of HP-TlB_3O_5 calculated by the CHARDI- and the BL/BS-concept.

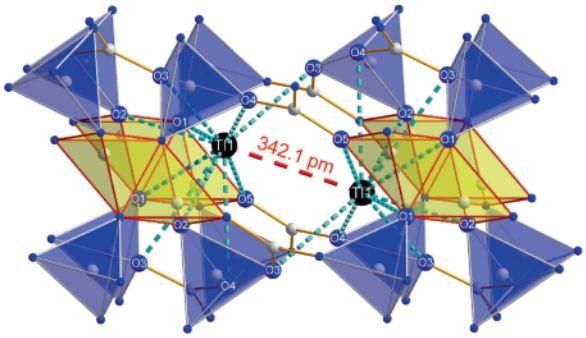

Fig. 4 (color online). Coordination of the Tl1 ion (short dashed bonds) in HP-TlB_3O_5 together with the distance to the neighboring Tl1 atom (long dashed line).

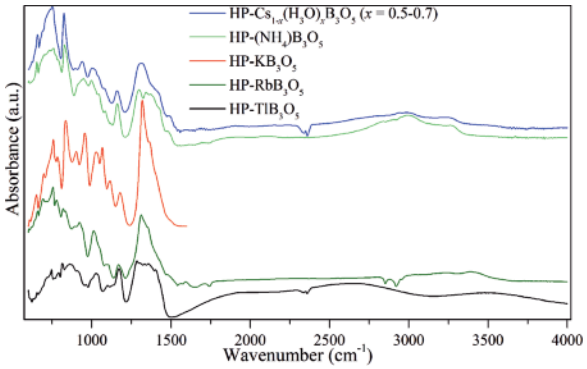

Fig. 5 (color online). Single-crystal IR spectra of HP-MB_3O_5 [$M = Cs_{1-x}(H_3O)_x$ ($x = 0.5-0.7$), NH_4, K, Rb, Tl] (top to bottom).

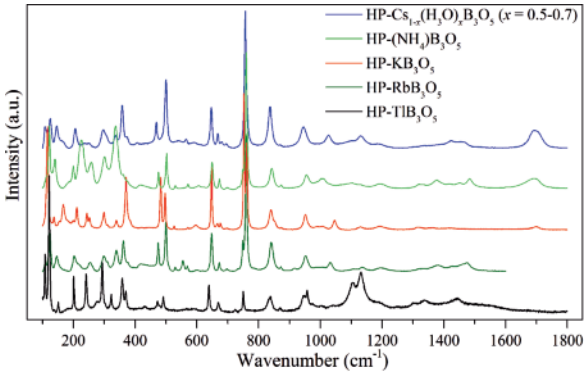

Fig. 6 (color online). Single-crystal Raman spectra of HP-MB_3O_5 [$M = Cs_{1-x}(H_3O)_x$ ($x = 0.5-0.7$), NH_4, K, Rb, Tl] (top to bottom).

parameter pressure at which the phase is formed also affects the lone pair effect.

The MAPLE values (*Ma*delung *P*art of *L*attice *E*nergy) [40–42] of HP-TlB_3O_5 were calculated and compared with the MAPLE values received from the summation of the binary components Tl_2O [43, 44] and B_2O_3-II [45]. The value of 34 203 kJ mol^{-1} was obtained in comparison to 34 132 kJ mol^{-1} (deviation = 0.21 %), starting from the binary oxides [Tl_2O (1225 kJ mol^{-1}) and B_2O_3-II (21 938 kJ mol^{-1})].

The bond valence sums of the atoms in the structure of HP-TlB_3O_5 were calculated from the crystal structure, using the bond length/bond strength concept (ΣV) [46, 47] and the CHARDI (*Char*ge *Di*stribution in Solids, ΣQ) concept [48, 49]. The results of the calculation are listed in Table 7 and fit to the values calculated for HP-$M'B_3O_5$ (M' = K, Rb).

Vibrational spectroscopy

The IR and the Raman spectra of HP-MB_3O_5 ($M = Cs_{1-x}(H_3O)_x$ ($x = 0.5-0.7$), NH_4, K, Rb, Tl) are compared in Figs. 5 and 6, respectively. A great similarity between the spectra of the different phases is obvious. In borates with different structural elements, bands between 800 and 1100 cm^{-1} are usually assigned to stretching modes of boron being tetrahedrally coordinated by oxygen atoms [50, 51], while absorption bands at 1200–1450 cm^{-1} are expected for borates containing BO_3 groups [51, 52].

A more specific assignment of the bands is possible by calculating the harmonic vibrational frequencies at the Γ point. These calculations were conducted for HP-KB_3O_5 [14]. According to these calculations, mainly the corner-sharing BO_3 groups are oscillating above 1320 cm^{-1}. Between 1215 and 950 cm^{-1}, stretching vibrations of the corner- and edge-sharing BO_4 tetrahedra occur. Bending and complex vibrations of both BO_3 and BO_4 units are located between 905 and 200 cm^{-1}. Below 185 cm^{-1}, lattice vibrations involving the alkali or pseudoalkali metal ions occur.

In the IR spectra of the phases HP-MB_3O_5 ($M = Cs_{1-x}(H_3O)_x$ ($x = 0.5-0.7$), NH_4, K, Rb, Tl),

the boron-oxygen tetrahedra within the structure are represented by several absorption bands between 700 and 1135 cm^{-1}. The BO_3 modes are detected between 1250 and 1500 cm^{-1}. The absorption above 1750 cm^{-1} in the IR spectrum of HP-TlB_3O_5 is an effect of the measurement. The beam is double-reflected in the measured crystal, and there is interference with the unreflected beam, leading to an oscillation in the intensity depending on the wavelength. Based on the resulting maxima and minima in the range 2600 – 5800 cm^{-1}, a crystal size of 0.0031 mm can be calculated from the IR measurement, assuming a refraction index of 1.7 [53]. Lattice vibrations appear in the Raman spectrum between 100 and 185 cm^{-1}. Complex and bending vibrations of BO_3 and BO_4 groups are located at 200 to 700 cm^{-1} and vibrations of the BO_4 tetrahedra at 950 to 1215 cm^{-1}. Above 1215 cm^{-1}, the BO_3 groups oscillate. All boron-oxygen units are linked to other boron-oxygen units, and thus every motion of one boron-oxygen unit induces motions in the surrounding units. However, according to calculations for HP-KB_3O_5, the edge-sharing tetrahedra oscillate around 1001, 1070 and 1105 cm^{-1} (IR-active) and 1013, 1161, 1205, and 1213 cm^{-1} (Raman-active) [14].

Conclusions

Single crystals of HP-TlB_3O_5 were synthesized at 6 GPa and 1400°C. Single-crystal X-ray diffraction data revealed a structure isotypic to HP-$M'B_3O_5$ (M' = K, Rb). With BO_3 groups and corner- and edge-sharing BO_4 tetrahedra, all basic structural motifs are present in the three-dimensional network. The IR and Raman spectra show great similarities to the isotypic phases. Unlike normal-pressure TlB_3O_5, any lone pair effect is present in the structure of HP-TlB_3O_5 at all.

Acknowledgement

Special thanks go to Univ.-Prof. Dr. R. Stalder (University of Innsbruck) for access to the IR spectrometer and to Dr. G. Heymann (University of Innsbruck) for the recording of the single-crystal data set.

[1] Y. Wu, J. Y. Yao, J. X. Zhang, P. Z. Fu, Y. C. Wu, *Acta Crystallogr.* **2010**, *E66*, i45.
[2] L. Yang, W. Fan, Y. Li, H. Sun, L. Wei, X. Cheng, X. Zhao, *Inorg. Chem.* **2012**, *51*, 6762 – 6770.
[3] S. Jin, G. Cai, W. Wang, M. He, S. Wang, X. Chen, *Angew. Chem. Int. Ed.* **2010**, *49*, 4967 – 4970.
[4] X. Chen, Y. Chen, C. Sun, X. Chang, W. Xiao, *J. Alloys Compd.* **2013**, *568*, 60 – 67.
[5] H. Huppertz, *Z. Naturforsch.* **2003**, *58b*, 278 – 290.
[6] H. Emme, H. Huppertz, *Acta Crystallogr.* **2005**, *C61*, i29–i31.
[7] H. Emme, H. Huppertz, *Chem. Eur. J.* **2003**, *9*, 3623 – 3633.
[8] S. C. Neumair, R. Kaindl, H. Huppertz, *Z. Naturforsch.* **2010**, *65b*, 1311 – 1317.
[9] J. S. Knyrim, F. Roessner, S. Jakob, D. Johrendt, I. Kinski, R. Glaum, H. Huppertz, *Angew. Chem. Int. Ed.* **2007**, *46*, 9097 – 9100.
[10] S. C. Neumair, R. Glaum, H. Huppertz, *Z. Naturforsch.* **2009**, *64b*, 883 – 890.
[11] S. C. Neumair, R. Kaindl, H. Huppertz, *J. Solid State Chem.* **2012**, *185*, 1 – 9.
[12] S. C. Neumair, S. Vanicek, R. Kaindl, D. M. Többens, K. Wurst, H. Huppertz, *J. Solid State Chem.* **2011**, *184*, 2490 – 2497.
[13] S. C. Neumair, G. Sohr, S. Vanicek, K. Wurst, R. Kaindl, H. Huppertz, *Z. Anorg. Allg. Chem.* **2012**, *638*, 81 – 87.
[14] S. C. Neumair, S. Vanicek, R. Kaindl, D. M. Többens, C. Martineau, F. Taulelle, J. Senker, H. Huppertz, *Eur. J. Inorg. Chem.* **2011**, 4147 – 4152.
[15] G. Sohr, S. C. Neumair, H. Huppertz, *Z. Naturforsch.* **2012**, *67b*, 1197 – 1204.
[16] G. Sohr, D. M. Többens, J. Schmedt auf der Günne, *Chem. Eur. J.* **2014**, *20*, in press.
[17] G. Sohr, S. C. Neumair, G. Heymann, K. Wurst, J. Schmedt auf der Günne, H. Huppertz, *Chem. Eur. J.* **2014**, *20*, 4316 – 4323.
[18] G. Sohr, D. Wilhelm, D. Vitzthum, M. K. Schmitt, H. Huppertz, *Z. Anorg. Allg. Chem.* **2014**, *640*, DOI: 10.002/zaac.201400312.
[19] N. Penin, L. Seguin, B. Gérand, M. Touboul, G. Nowogrocki, *J. Solid State Chem.* **2001**, *160*, 139 – 146.
[20] M. Touboul, G. Nowogrocki, *J. Solid State Chem.* **1998**, *136*, 216 – 220.
[21] M. Touboul, E. Bétourné, G. Nowogrocki, *J. Solid State Chem.* **1997**, *131*, 370 – 373.
[22] M. Touboul, D. Amoussou, *Rev. Chim. Minér.* **1978**, *15*, 223 – 232.

[23] R. Marchand, Y. Piffard, M. Tournoux, *C. R. Séances Acad. Sci., Sér. C* **1973**, *276*, 177 – 179.
[24] M. Touboul, D. Amoussou, *C. R. Séances Acad. Sci., Sér. C* **1977**, *285*, 145 – 147.
[25] M. Touboul, *Rev. Chim. Minér.* **1971**, *8*, 347 – 384.
[26] M. Touboul, R. Bouaziz, *C. R. Séances Acad. Sci., Sér. C* **1967**, *265*, 372 – 375.
[27] G. Canneri, R. Morelli, *Atti Accad. Naz. Lincei, Cl. Sci. Fis., Mat. Nat., Rend.* **1922**, *31*, 109 – 111.
[28] N. Kawai, S. Endo, *Rev. Sci. Instrum.* **1970**, *41*, 1178 – 1181.
[29] D. Walker, M. A. Carpenter, C. M. Hitch, *Am. Mineral.* **1990**, *75*, 1020 – 1028.
[30] D. Walker, *Am. Mineral.* **1991**, *76*, 1092 – 1100.
[31] H. Huppertz, *Z. Kristallogr.* **2004**, *219*, 330 – 338.
[32] STOE WIN XPOW INDEX, Stoe & Cie GmbH, Darmstadt (Germany), **2008**.
[33] Z. Otwinowski, W. Minor in *Methods in Enzymology*, Vol. 276, *Macromolecular Crystallography*, Part A (Eds.: C. W. Carter, Jr., R. M. Sweet), Academic Press, New York, **1997**, pp. 307 – 326.
[34] G. M. Sheldrick, *Acta Crystallogr.* **2008**, *A64*, 112 – 122.
[35] G. M. Sheldrick, SHELXL, Crystal Structure Refinement, Multi-CPU Version, University of Göttingen, Göttingen (Germany), **2013**.
[36] T. Gruene, H. W. Hahn, A. V. Luebben, F. Meilleur, G. M. Sheldrick, *J. Appl. Crystallogr.* **2014**, *47*, 462 – 466.
[37] LABSPEC, Horiba Jobin Yvon S. A. S., Villeneuve d'Ascq (France), **2010**.
[38] A. Neuhaus, *Chimia* **1964**, *18*, 93 – 103.
[39] J. Krogh-Moe, *Acta Crystallogr.* **1974**, *B30*, 1178 – 1180.
[40] R. Hoppe, *Angew. Chem., Int. Ed. Engl.* **1966**, *5*, 95 – 106.
[41] R. Hoppe, *Angew. Chem., Int. Ed. Engl.* **1970**, *9*, 25 – 34.
[42] R. Hübenthal, MAPLE, Program for the Calculation of MAPLE Values, University of Gießen, Gießen (Germany), **1993**.
[43] P. Touzain, M. Caillet, *Rev. Chim. Minér.* **1971**, *8*, 277 – 286.
[44] G. H. Kwei, M. A. Subramanian, *Physica C* **1990**, *168*, 521 – 529.
[45] C. T. Prewitt, R. D. Shannon, *Acta Crystallogr.* **1968**, *B24*, 869 – 874.
[46] N. E. Brese, M. O'Keeffe, *Acta Crystallogr.* **1991**, *B47*, 192 – 197.
[47] I. D. Brown, D. Altermatt, *Acta Crystallogr.* **1985**, *B41*, 244 – 247.
[48] R. Hoppe, *Z. Kristallogr.* **1979**, *150*, 23 – 52.
[49] R. Hoppe, S. Voigt, H. Glaum, J. Kissel, H. P. Müller, K. Bernet, *J. Less-Common Met.* **1989**, *156*, 105 – 122.
[50] J. P. Laperches, P. Tarte, *Spectrochim. Acta* **1966**, *22*, 1201 – 1210.
[51] M. Ren, J. H. Lin, Y. Dong, L. Q. Yang, M. Z. Su, L. P. You, *Chem. Mater.* **1999**, *11*, 1576 – 1580.
[52] W. C. Steele, J. C. Decius, *J. Chem. Phys.* **1956**, *25*, 1184 – 1188.
[53] OPUS, Bruker Optik GmbH, Ettlingen (Germany), **2008**.